Dye Transfer between Surfactant-Free Nanodroplets Dispersed in Water

Toshio Sakai,[†] Yoshihiro Takeda,[‡] Fumitaka Mafuné,[§] Masahiko Abe,[†] and Tamotsu Kondow*[,§]

Faculty of Science and Technology, Tokyo University of Science, 2641 Yamazaki, Noda, Chiba 278-8510, Japan, Genesis Research Institute, Inc., 717-86 Futamata, Ichikawa, Chiba 272-0001, Japan, and Cluster Research Laboratory, Toyota Technological Institute, 717-86 Futamata, Ichikawa, Chiba 272-0001, Japan

Received: December 12, 2001; In Final Form: March 1, 2002

A single nanodroplet of *n*-decane in a surfactant-free *n*-decane-in-water emulsion was detected by observing fluorescence emitted from C540 dye molecules dissolved in the droplet on the basis of confocal fluorescence microscopy. The fluorescence intensity was found to decrease when a dye-free *n*-decane-in-water emulsion was added, because the dye molecules are transferred to the dye-free droplets. Insensitive change of the rate of the dye transfer with the amount of the dye-free emulsion added to the dye-containing one is explained in such a manner that the permeation of the dye molecules across the droplet−water interface is the rate-determining step. The rate-decrease with the diameter of the droplet reveals that the permeability and solubility of the dye molecules into the droplet tends to increase with the droplet diameter.

Introduction

A surfactant-free emulsion has been investigated because it provides genuine information on the fundamental properties that the emulsion itself has;[1−5] in surfactant-stabilized emulsions, the effect of the surfactant should be taken into account. In the studies of such surfactant-free emulsions, it is important to elucidate the behaviors of the constituent droplets such as droplet growth and mass transfer among different droplets. Particularly, the mechanism of the mass transfer ought to be clarified in relation to construction of a material delivery system by taking advantage of the mass transfer activity of the droplets. In general, the overall mass transfer rate depends critically on the permeation rate of a molecule of interest across the droplet-liquid interface, the diffusion rate of the molecule in the liquid medium, the adsorption and the desorption rates of the molecule on the droplet surface, the solvent reorganization rate, the rate of a complex formation, etc.[6−10] Many investigations have been reported so far in this relation. For instance, interfacial mass transfer processes involving droplets having a submicrometer in diameter have been studied by measuring the rates of the mass transfer processes with macroscopic techniques such as solvent extraction in emulsions. Further, spectroscopic and electrochemical techniques in combination with laser trapping have been applied to measure the mass transfer rate across the surface of a single droplet.[11−18]

With decrease in the droplet diameter as low as nanometers, a fundamental change in the droplet properties is expected to occur as reported in the studies of nanoparticles and clusters.[19−24] In this context, the mass transfer rate involving a droplet (nanodroplet) having a nanometer in diameter should change remarkably with its diameter and provide crucial information on how the droplets trap and release molecules of interest. However, no practical methodology is available for the detection of nanodroplets. In the present study, detection of a dye-labeled single emulsion droplet in water was achieved, and the mass transfer rate across the droplet surface was measured as a function of the droplet diameter.

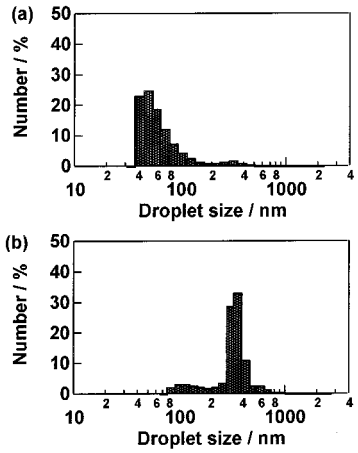

Figure 1. Size distributions of freshly prepared *n*-decane droplets (a) and those 2 h after preparation (b), which are determined by dynamic light scattering measurements.

Experimental Section

Materials and Sample Preparation. An emulsion was prepared by mixing *n*-decane (GR grade, Tokyo Kasei Co., Ltd.) dissolving 1×10^{-5} mol L^{-1} of coumarin 540 (C540; laser grade, Exciton, Inc.) and deionized water (Ohtsuka Pharmacy Co., Ltd.) by an ultrasonic cleaner (FU-10C, 60 W, 28 kHz, Tokyo Garasu Kikai Co., Ltd.). The concentrations of *n*-decane and the dye in the water turn out to be 5×10^{-4} mol L^{-1} and $\sim 1 \times 10^{-9}$ mol L^{-1}, respectively. Figure 1 shows droplet size distributions of the *n*-decane emulsion measured by the dynamic light scattering method; panels (a) and (b) are the distributions

* Author to whom correspondence should be addressed. Phone: +81-47-320-5911. Fax: +81-47-327-8031. E-mail: kondow@mail.cluster-uni-t.ocn.ne.jp.
[†] Tokyo University of Science.
[‡] Genesis Research Institute, Inc.
[§] Toyota Technological Institute.

10.1021/jp014503i CCC: $22.00
Published on Web 04/19/2002

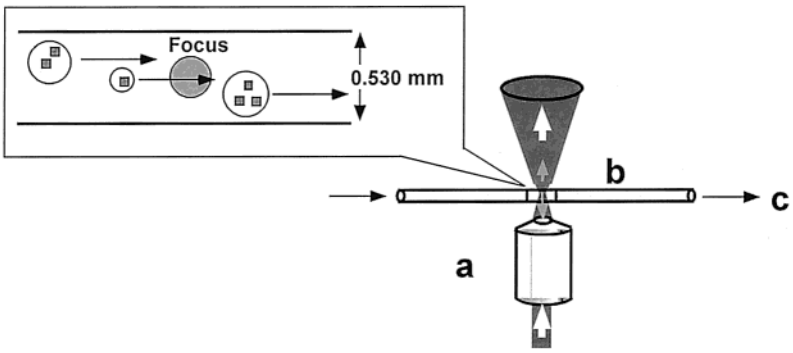

Figure 2. Schematic drawing of a core section of the apparatus. Objective lens (a), capillary (b), and flow of a sampling liquid (c).

of a freshly prepared emulsion containing *n*-decane droplets with the average diameter of 50 nm and that (average diameter of 300 nm) observed 2 h after the preparation, respectively.

Single Droplet Detection. The number of C540 molecules contained in a single droplet was estimated from the fluorescence intensity of the dye molecules, which was measured by a confocal fluorescence microscope (IX70,OLYMPUS) at the ambient temperature of 23 ± 1 °C (see Figure 2). The sample solution was allowed to flow through a glass capillary with 0.530 mm in the inner diameter at a flow rate of $\sim 1.06 \times 10^{-3}$ L min^{-1} by a pump. The flow rate was minimized so as to maximize the detection efficiency, as discussed in the following section. The lowest limit of the flow rate was so set that the emulsion droplets flow too fast to adsorb on the inner surface of the capillary. The capillary tube was placed right above an objective lens (UplanApo 100 × Oil I, OLYMPUS) of the microscope. An argon ion laser (BeamLok 2060-7S; Spectra-Physics, Co.) was illuminated to excite C540 molecules in a single droplet at the wavelength of 476.5 nm. The fluorescence of C540 molecules in a single droplet passing through the focal volume of the laser beam was collected by the same objective lens and served for focusing the excitation laser. After removing Rayleigh scattering by the droplets and Raman scattering from water by using band-pass filters (above 515 nm and 520−550 nm), the fluorescence was detected by an avalanche photodiode having a quantum efficiency of 70%. The fluorescence signal from the detector was processed and registered in a multichannel counter (Stanford Research Systems, SR430) based on a personal computer (Gateway 2000, G6-200). In the confocal configuration, a pinhole with a 20 μm diameter was located at the conjugated position in front of the photodiode. The fluorescence was so focused at the pinhole that the fluorescence from the focal volume was maximized, and otherwise minimized by defocusing at the pinhole. The focal volume was found to be 1 μm in depth and 0.8 μm in diameter and hence the focal volume turns out to be $\sim 5 \times 10^{-16}$ L.

Results

Emulsion A containing 5×10^{-4} mol L^{-1} of C540-labeled droplets having an average diameter of 300 nm was mixed with the same amount of emulsion B containing 5×10^{-4} mol L^{-1} of dye-free droplets having the same average diameter, and the time evolution was observed after the mixing. Figure 3 a shows the time evolution of the fluorescence signal with the gate time of 82 μs from individual C540-labeled droplets in emulsion A, which are flowing through the focal volume of the confocal fluorescence microscope. As argued in the Experimental section, each spike-like signal (bunching signal) arises from a single droplet containing C540 molecules, and its height gives rises to the number of the C540 molecules. Figure 3, parts b and c,

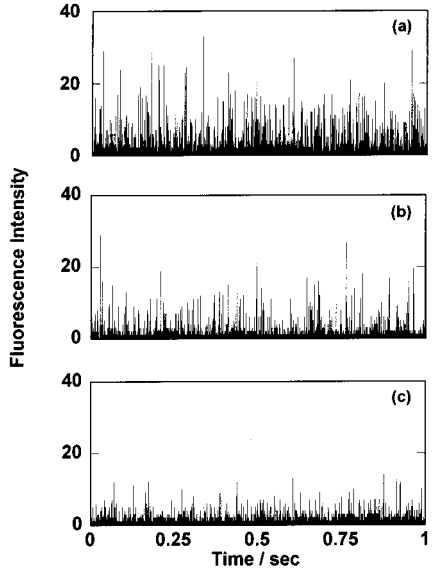

Figure 3. Time evolution of fluorescence bunching signals just after the equal-volume mixing of emulsion B to emulsion A (a), at 30 s (b), and at 300 s (c) after the mixing.

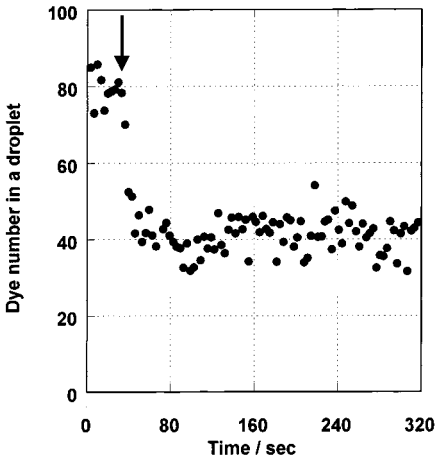

Figure 4. Average number of C540 molecules per droplet is plotted as a function of the elapsed time after equal-volume mixing of emulsion A with emulsion B. The arrow indicates the time of the mixing.

show the time evolutions of the fluorescence signal for the mixture of emulsions A and B at 30 and 300 s after the mixing. The average height of the bunching signals, which gives the average number of C540 molecules per droplet, decreases with the elapsed time after the mixing.

Figure 4 shows the average height of the bunching signals plotted against the elapsed time. Note that the average height is converted (see the Experimental section) to the average

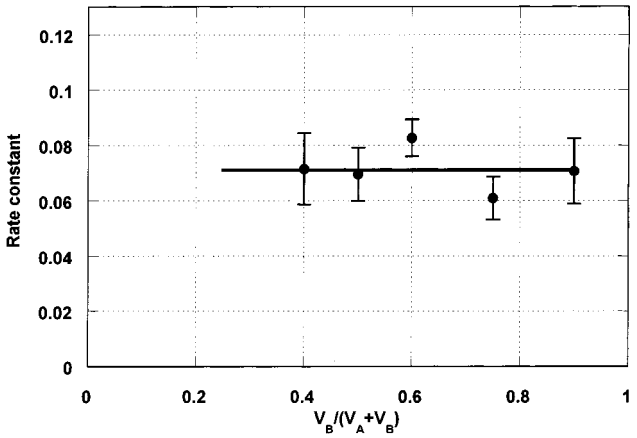

Figure 5. Rate constants plotted as a function of the volume fraction of $V_B/(V_A + V_B)$, where V_X represents the volume of emulsion X (X = A or B). The solid line shows the result obtained by least-squares fitting of eq 13.

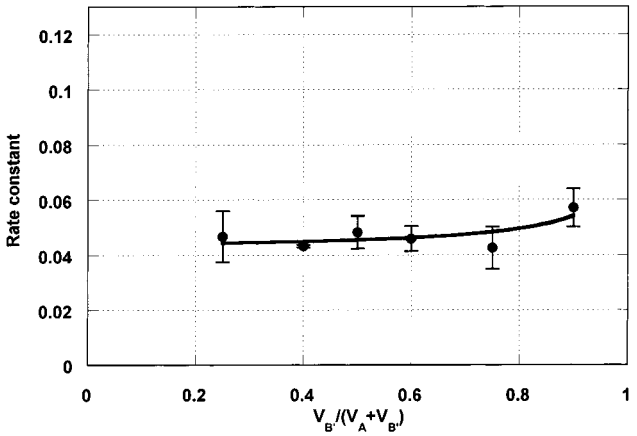

Figure 6. Rate constants plotted as a function of the volume fraction of $V_{B'}/(V_A + V_{B'})$, where V_X represents the volume of emulsion X (X = A or B′). Emulsion B′ contains almost the same number density of dye-free droplets having the average diameter of 50 nm. The solid line shows the result obtained by least-squares fitting of eq 10.

number of C540 molecules per droplet. The number density of detectable droplets decreases rapidly within 10 s after mixing the same amount of emulsion A with emulsion B containing only dye-free droplets. Concurrently the average number of C540 molecules per droplet decreases with the elapsed time. As a comparison, the same measurement was performed but mixing with water instead of emulsion B. No change in the number of C540 molecules per droplet was observed although the number density of detectable droplets dropped similarly. These findings indicate that C540 molecules dissolved in droplets are transferred to dye-free droplets introduced into the water afterward; *dye transfer*.

To examine the mechanism of the dye transfer, the rate constant of the dye transfer process was obtained from the initial decrease of the average height of the bunching signals on the assumption that the initial decrease in the average height is expressed as an exponential function with the rate constant of the dye transfer; as described in the Discussion section this assumption is verified by the scheme proposed. The rate constant thus obtained was found to depend on the mixing ratio of emulsion A with emulsion B. Figure 5 shows the rate constant plotted against $V_B/(V_A + V_B)$, where V_X represents the total volume of droplets in emulsion X (X = A or B) used for preparing the mixture. A similar measurement of mixing emulsion A with emulsion B′ was performed, where emulsion B′ contains almost the same number density of dye-free droplets having the average diameter of 50 nm. Figure 6 shows the rate constant plotted against $V_{B'}/(V_A + V_{B'})$.

Discussion

Condition of Single Droplet Detection. Let us evaluate the highest concentration limit below which the single droplet detection is achieved. Suppose that the probability, $f(k)$, for k droplets being inside the focal volume is given by a Poisson distribution,

$$f(k) = e^{-np}\frac{(np)^k}{k!} \quad (1)$$

where n and p represent a droplet concentration (L^{-1}) and a volume of a focusing region (L), respectively. The initial droplet concentration is obtained from the volume of *n*-decane mixed initially with water and the distribution of the diameters of freshly prepared droplets as shown in Figure 1a. At a droplet concentration less than 10^{-9} mol L^{-1}, the single droplet detection is achieved because the probability for finding more than 2 droplets in the focal volume is calculated to be negligibly small.

Fluorescence Signal from a Single Droplet. Under irradiation of the 476.5 nm laser, a C540 molecule in a single droplet emits $\sim 10^8$ photons (s^{-1}) in a wavelength of 480−550 nm by repeating absorption and fluorescence cycles. In this single-droplet detection experiment, a C540-labeled single droplet flows through the focal volume and emits photons. The intensity of the bunching fluorescence signal should be proportional to the number of the C540 molecules in the droplet. The residence time of the droplet in the focal volume is ~ 10 μs at the flow velocity of $\sim 1.06 \times 10^{-3}$ L min^{-1} in the glass capillary. It follows that, for each C540 molecule traversing across the focal volume, it fluoresces less than 10 photon-counts and typically 2−3 photon-counts with taking the quantum efficiency ($\sim$1%) of the detector into account. As described in the Results section, a single droplet traversing the focal volume of the microscope provides a single bunching fluorescence signal as shown in Figure 3. Fluorescence from C540 molecules dissolved in water can be disregarded, because of its negligibly small solubility in water. In the initial stage of the dye transfer from C540-labeled droplets, the droplets of emulsion B give practically no contribution to the bunching signals by considering the efficiency of the detector.

Dye Transfer between Droplets. As stated in the Results section, C540 molecules in a droplet are transferred to the other droplets (dye transfer). Although the dye transfer proceeds between dye-labeled droplets and between dye-free droplets, these processes are not taken into account in the analysis. Therefore, the rate observed corresponds to that of the dye transfer between dye-labeled and dye-free droplets. Let us assume that C540 molecules in C540-labeled droplets are being permeated into water and then into dye-free droplets as

$$\mathrm{A} \rightleftarrows \mathrm{W} \rightleftarrows \mathrm{B} \quad (2)$$

where A, W, and B represent emulsion A, water, and emulsion B, respectively, and arrows show the directions of C540 molecules. The following equations are obtained from eq 2 in terms of the rates of the dye transfer, d[A]/dt, d[B]/dt, and d[W]/dt related to A, W, and B, respectively, where [X] represents the concentration of C540 in X. The equations are

$$V_A\, \mathrm{d[A]/d}t = -(3V_A/r_a)P_a[\mathrm{A}] + (3V_A/r_a)P_{-a}[\mathrm{W}] \quad (3)$$

$$V_W\, d[W]/dt = (3V_A/r_a)P_a[A] - (3V_A/r_a)P_{-a}[W] - (3V_B/r_b)P_{-b}[W] + (3V_B/r_b)P_b[B] \quad (4)$$

$$V_B\, d[B]/dt = (3V_B/r_b)P_{-b}[W] - (3V_B/r_b)P_b[B] \quad (5)$$

where V_A, V_B, and V_W are the volumes of emulsion A, B, and water, respectively, r_a and r_b are the radii of a C540-labeled and a dye-free droplet, respectively, and P_a and P_{-a} are the permeability coefficient of a C540 molecule from a C540-labeled droplet to water and that of the reverse direction, respectively, and P_b and P_{-b} are the permeability coefficients related to a dye-free droplet vs water. In the steady-state approximation with $d[W]/dt = 0$, one obtains

$$[W] = ((3V_A/r_a)\,P_a[A] + (3V_B/r_b)\,P_b[B])/((3V_A/r_a)\,P_{-a} + (3V_B/r_b)\,P_{-b}) \quad (6)$$

The conservation of the total number of C540 molecules in the dye transfer gives

$$V_B[B] = V_A([A]_0 - [A]) - V_W[W] \quad (7)$$

where $[A]_0$ is the initial C 540 concentration in emulsion A. Taking all the relations into account, one obtains

$$d[A]/dt = -\alpha[A] + \beta[A]_0 \quad (8)$$

where

$$\alpha = 3\,(P_bP_{-a}V_A + P_aP_{-b}V_B + P_aP_bV_W)/(r_bP_{-a}V_A + r_aP_{-b}V_B + r_aP_bV_W) \quad (9)$$

$$= (3/r_a)\,P_a + (3/r_a)\,P_{-a}\,(r_aP_b - r_bP_a)\,V_A/(r_bP_{-a}V_A + r_aP_{-b}V_B + r_aP_bV_W) \quad (10)$$

$$\beta = 3P_{-a}P_bV_A/(r_bP_{-a}V_A + r_aP_{-b}V_B + r_aP_bV_W) \quad (11)$$

The average concentration of C540 molecules in emulsion A is given by

$$[A] = ((\alpha - \beta)/\alpha)\,[A]_0 \exp(-\alpha t) + (\beta/\alpha)\,[A]_0 \quad (12)$$

As shown in eq 12, the concentration exponentially decreases with the elapsed time after mixing, where α corresponds to the rate constant of the dye transfer. In the initial stage of the dye transfer, a number of C540 molecules in a droplet in emulsion B is not significantly large, so that the fluorescence signals of the droplets in emulsion B can be disregarded. By taking this into consideration, the rate constant of the dye transfer was obtained from several data points in the initial stage of the mixing.

Mixing Ratio Dependence. To examine the validity of the present scheme for the dye transfer, we examined how the rate constant, α, of the dye transfer depends on the mixing ratio $V_B/(V_A + V_B)$. As shown in Figure 5, the dye-transfer rate, α, is almost independent of $V_B/(V_A + V_B)$. This finding agrees with the prediction given by the proposed scheme as follows: The dynamics of the dye-molecule transfer between A and W is identical with that between B and W, because the average radius of droplets in emulsion B is the same as that in emulsion A ($r_a = r_b = r$). It follows that the permeability coefficients, P_b and P_{-b} are equal to P_a ($= P_+$) and P_{-a}($= P_-$), respectively, and the dye transfer rate, α, is simplified as

$$\alpha = (3/r)\,P_a \quad (13)$$

Namely, the rate constant of the dye transfer does not depend on the mixing ratio. Equation 13 gives the permeability coefficient, P_a ($= P_+$), of $(3.6 \pm 0.6) \times 10^{-9}$ m s^{-1} by introducing the rate constant, α, of $(7.1 \pm 0.4) \times 10^{-2}$ and the average radius, r, of 150 ± 25 nm. As described above, no decrease of C540 molecules in the droplets of emulsion A is observed even if emulsion A is diluted with water. This result implies that P_- is more than 4 orders of magnitude larger than P_+. Note that V_W is typically 4 orders of magnitude larger than V_A.

As mentioned so far, the dynamics of the dye transfer between the droplets is explained in terms of permeation of the dye molecules into water and then into the dye-free droplets. The dye transfer by the collision of the droplets is regarded as a minor process, because the rate constants of the dye transfer do not depend on the collision frequency of the emulsion droplets. If the dye transfer were controlled by the collision processes, the rate constants could change with $n_An_B/(n_A + n_B)$ where n_A and n_B are the number of the droplets of emulsion A and B, and hence the rate constants should show a maximum at the 0.5 mixing ratio of emulsion A and B. This result implies that the dye transfer is not controlled by collision processes, but by permeation of the dye molecules into water and then into dye-free droplets.

Size Dependence. As described in the Results section, we also measured the rate constant of the dye transfer by mixing emulsion A with emulsion B′ consisting of dye-free droplets having the average diameter of ~50 nm. The rate constant depends on the mixing ratio, $V_{B'}/(V_A + V_{B'})$, and is smaller than that for dye-free droplets with the average diameter ~300 nm (see Figure 6). Using eq 10 with leaving P_{-a}, P_b, and P_{-b} as the variable parameters, one obtains P_{-a}, P_b, and P_{-b} to be 1.3×10^{-3}, 3.5×10^{-10}, and 1.0×10^{-5} m s^{-1}, respectively, where P_a is approximated by P_+ for a droplet with the diameter of ~300 nm. In summary, the permeability coefficient has a tendency of decreasing with decrease in the diameter. In other words, C540 molecules in a 300-nm droplet permeate water more rapidly than those in a 50-nm droplet do. The phenomenon is explained in terms of the surface structure of the droplets and hydrogen-bonding of the interfacial water molecules. A number of OH^- adhere on the surface of the droplets and the interfacial water molecules are tightly bound to OH^-. Actually, the degree of hydrogen-bonding of OH^- with water molecules on the droplet surface has been measured as surface potential, and the origin of the surface potential at the oil−water interface is known to be the strong dipole moment or the hydrogen-bonding of the OH^- ions with the hydrogen atoms of the interfacial water molecules.[25,26] Indeed, the surfactant-free *n*-decane droplets with diameter of 50 nm have a negative surface potential (ζ-potential) around −45 mV and the potential decreases with increase in the droplet size.[27] Namely, the number of the OH^- ions interacting with the hydrogen atom of the interfacial water molecules per unit surface area decreases with an increase in the droplet size. The more tight hydrogen-bonding network must be formed around the smaller droplets, because of the higher density of OH^- ions. The network hinders C540 molecules permeating water, and vice versa.

The solubility of C540 molecules in a droplet, which is given by the ratio P_-/P_+, turns out to be 3.6×10^5 for the average diameter of 300 nm and 2.8×10^4 for 50 nm. The decrease of the solubility is much larger than that expected from a picture that a solute molecule in a solution is stabilized by a solvation shell with a diameter of ~1 nm. In a small droplet, a long-

range interaction such as that from the curved droplet surface can operate for the stabilization of C540 molecules.

Conclusion

We developed a single-particle detection technique based on confocal fluorescence microscopy, and thereby individual droplets dispersed in water were detected without any help of laser trapping, etc. One of the outstanding features of this technique is the capability of real-time observation of nanodroplets and monitoring of a dye transfer process. We successfully observed the dye transfer process among decane nanodroplets dispersed in water by applying this single-particle detection technique and revealed that larger nanodroplets trap and release the dye molecules more readily than a smaller one does. This finding suggests that the fundamental properties of liquid droplets in a liquid medium change remarkably with their diameters, especially in a nanometer range.

Acknowledgment. The authors are indebted to Professor R. N. Zare and Professor D. T. Chiu for the technical advise for the single molecule detection method. This work was supported by the Cluster Research Project of the Genesis Research Institute, Inc.

References and Notes

(1) Kamogawa, K.; Sakai, T.; Momozawa, N.; Shimazaki, M.; Enomura, M.; Sakai, H.; Abe, M. *J. Jpn. Oil Chem. Soc.* **1998**, *47* (2), 159.

(2) Kamogawa, K.; Matsumoto, M.; Kobayashi, T.; Sakai, T.; Sakai, H.; Abe, M. *Langmuir* **1999**, *15* (6), 1913.

(3) Kamogawa, K.; Akatsuka, H.; Matsumoto, M.; Yokoyama, S.; Sakai, T.; Sakai, H.; Abe, M. *Colloids Surf., A: Physicochem. Eng. Aspects* **2001**, *180*, 41.

(4) Sakai, T.; Kamogawa, K.; Harusawa, F.; Momozawa, N.; Sakai, H.; Abe, M. *Langmuir* **2001**, *17* (2), 255.

(5) Sakai, T.; Kamogawa, Kwon, K. O.; Sakai, H.; Abe, M. *Colloid Polym. Sci.* **2002**, *280* (2), 99.

(6) Christian, S. D.; Smith, G. A.; Tucker, E. E. *Langmuir* **1985**, *1*, 564.

(7) Rupert, L. A. M.; Engberts, J. B. F. N.; Hoekstra, D. *J. Am. Chem. Soc.* **1986**, *108* (14), 3920.

(8) Kondo, Y.; Abe, M.; Ogino, K.; Uchiyama, H.; Scamehorn, J. F.; Tucher, E. E.; Christian, S. D. *Langmuir* **1993**, *9*, 899.

(9) You, H.; Tirrell, D. A. *J. Am. Chem. Soc.* **1991**, *113* (10), 1023.

(10) DiTizio, V.; Karlgard, C.; Lilge, L.; Khourt, A. E.; Mittelman, M. W.; DiCosmo, F. *J. Biomed. Mater. Res.* **2000**, *51* (1), 96.

(11) Nakatani, K.; Chikama, K.; Kim, H.-B.; Kitamura, N. *Chem. Lett.* **1994**, *4*, 793.

(12) Nakatani, K.; Chikama, K.; Kim, H.-B.; Kitamura, N. *Chem. Phys. Lett.* **1995**, *237* (1, 2), 133.

(13) Nakatani, K.; Wakabayashi, M.; Chikama, K.; Kitamura, N. *J. Phys. Chem.* **1996**, *100* (16), 6749.

(14) Chikama, K.; Nakatani, K.; Kitamura, N. *Chem. Lett.* **1996**, *8*, 665.

(15) Chikama, K.; Nakatani, K.; Kitamura, N. *Bull. Chem. Soc. Jpn.* **1998**, *71* (5), 1065.

(16) Nakatani, K.; Chikama, K.; Kitamura, N. *Adv. Photochem.* **1999**, *25*, 173.

(17) Chiu, D. T.; Lillard, S. J.; Scheller, R. H.; Zare, R. N. *Science* **1998**, *279*, 1190.

(18) Stromberg, A.; Ryttsen, F.; Chiu, D. T.; Davidson, M.; Eriksson, P. S.; Wilson, C. F.; Prwar, O.; Zare, R. N. *PNAS* **2000**, *97*, 7.

(19) Heiz, U.; Vanolli, F.; Sanchez, A.; Schneider, W.-D. *J. Am. Chem. Soc.* **1998**, *120*, 9668.

(20) Fayet, P.; Granzer, F.; Hegenbart, G.; Mooisar, E.; Pischel, B.; Woeste, L. *Z. Phys. D: At., Mol. Clusters* **1986**, *3*, 299.

(21) Bucher, J. P.; Box, A. J.; Douglass, D. C.; Boomfield, L. A. *Phys. Rev. B* **1993**, *47*, 12874.

(22) Wilcoxon, J. P.; Martin, J. E.; Parsapour, F.; Wiedenman, B.; Kelley, D. F. *J. Chem. Phys.* **1998**, *108*, 9137.

(23) Haruta, M.; Tsubota, S.; Kobayashi, T.; Kageyama, H.; Genet, M. J.; Delmon, B. *J. Catal.* **1993**, *144*, 175.

(24) Ahmadi, T. S.; Logunov, S. L.; El-Sayed, M. A. *Nanostructured Materials*; Shalaev, V. M., Moskovits, M., Eds.; American Chemical Society: Washington, DC, 1997.

(25) Taylor, A. J.; Wood, F. W. *Trans. Faraday Soc.* **1957**, *53*, 523.

(26) Marinova, K. G.; Alargova, R. G.; Denkov, N. D.; Velev, O. D.; Petsev, D. N.; Ivanov, I. B.; Borwankar, R. P. *Langmuir* **1996**, *12*, 2045.

(27) Sakai, T.; Takada, Y.; Mafuné, F.; Abe, M.; Kondow, T. To be submitted.